Published in final edited form as:
J Immunol. 2013 September 1; 191(5): 2637–2646. doi:10.4049/jimmunol.1300082.

Role of RNase L in Viral PAMP/Influenza Virus and Cigarette Smoke-induced Inflammation and Remodeling

Yang Zhou[*], **Min-Jong Kang**[*], **Babal Kant Jha**[†], **Robert H. Silverman**[†], **Chun Geun Lee**[*], and **Jack A. Elias**[*]

[*]Section of Pulmonary and Critical Care Medicine and Department of Internal Medicine, Yale University School of Medicine, New Haven, CT 06520-8057

[†]Department of Cancer Biology, Lerner Research Institute, Cleveland Clinic, Cleveland, OH 44195 USA

Abstract

Interactions between cigarette smoke (CS) exposure and viral infection play an important role(s) in the pathogenesis of chronic obstructive pulmonary disease (COPD) and a variety of other disorders. A variety of lines of evidence suggest that this interaction induces exaggerated inflammatory, cytokine and tissue remodeling responses. We hypothesized that the 2′-5′OAS/RNase L system, an innate immune antiviral pathway, plays an important role in the pathogenesis of these exaggerated responses. To test this hypothesis we characterize the activation of 2′-5′ oligoadenylate synthase (OAS) in lungs from mice exposed to CS and viral PAMPs/live virus, alone and in combination. We also evaluated the inflammatory and remodeling responses induced by CS and virus/viral PAMPs in lungs from RNase L null and wild type mice. These studies demonstrate that CS and viral PAMPs/live virus interact in a synergistic manner to stimulate the production of select OAS moieties. They also demonstrate that RNase L plays a critical role in the pathogenesis of the exaggerated inflammatory, fibrotic, emphysematous, apoptotic, TGF-β1 and type I IFN responses induced by CS plus virus/viral PAMP in combination. These studies demonstrate that CS is an important regulator of antiviral innate immunity, highlight novel roles of RNase L in CS plus virus induced inflammation, tissue remodeling, apoptosis and cytokine elaboration and highlight pathways that may be operative in COPD and mechanistically-related disorders.

Introduction

Chronic obstructive pulmonary disease (COPD) is a composite term that encompasses chronic bronchitis and emphysema (1). It is the 4th leading cause of death in the world and, in Western societies, is strongly associated with cigarette smoke (CS) exposure (1). Chronic bronchitis is characterized by chronic inflammation and mucus metaplasia, while emphysema exhibits structural cell apoptosis and enlargement of alveolar airspace (1–3). Recent studies have also highlighted the interesting observation that the airways in COPD tissues are often remodeled and fibrotic while the nearby alveoli manifest tissue rarification and septal rupture (1). The inflammation in COPD tissues is felt to be causally related to the emphysema and other pathologic alterations in the lungs from these patients (1, 2, 4, 5) and worsens with disease progression (1, 4, 5). The mechanisms that mediate these inflammatory and remodeling responses, however, are not adequately understood.

Corresponding author: Jack A. Elias, M.D., Section of Pulmonary and Critical Care Medicine and Department of Internal Medicine, Yale University School of Medicine, New Haven, CT 06520-8057, Tel: 203-785-4119, Fax: 203-785-6954, jack.elias@yale.edu.

Acute exacerbations are a leading cause of morbidity and mortality in COPD (6) and bacterial and respiratory virus infections account for 50%–70% of these exacerbations (7, 8). When compared with other causes of COPD exacerbations those caused by viral upper respiratory tract infections are associated with more severe symptoms, more frequent hospitalizations, and longer recovery times (9, 10). Influenza virus, rhinovirus, coronavirus, respiratory syncytial virus, parainfluenza, adenovirus, and metapneumovirus are important causes of COPD exacerbations (4). The frequency of these exacerbations correlates with the rate of disease progression and loss of lung function as well as the overall health status of the patient (6–10). Thus, exacerbations are now considered to be legitimate targets for disease therapy (8, 9). However, the mechanisms that mediate these exacerbations and their effects on tissue inflammation and remodeling have not been adequately defined.

A number of lines of evidence have demonstrated that innate immune responses play important roles in the pathogenesis of COPD (11–14). In keeping with these findings and their clinical import, studies from our laboratory and others have investigated the effects of CS, viruses and viral pattern associated molecular patterns (PAMPs), alone and in combination, on pulmonary innate immunity. These studies demonstrated that CS and viruses/viral PAMPs interact in a synergistic manner to increase pulmonary inflammation and fibrotic and emphysematous tissue remodeling (5). They also demonstrated that these exaggerated responses are mediated by a MAVS (mitochondrial antiviral signaling molecule)-dependent cytokine cascade characterized by the early induction of type I interferon (IFN) and IL-18, later induction of IL-12/IL-23 p40 and IFN-γ (5). However, the possibility that other innate/antiviral pathways could also contribute to these responses has not been fully addressed.

Ribonuclease L (also called RNase L, ribonuclease 4 or 2–5A-dependent ribonuclease) is an interferon (IFN)-stimulated, highly regulated endoribonuclease that is widely expressed in mammalian tissues (15). It is produced as a latent enzyme, activated by OAS (2′-5′ oligoadenylatesynthetase) proteins and destroys cellular and viral RNAs (16). It is a major effector of IFN-induced antiviral responses that can inhibit the replication of a variety of viruses including encephalomyocarditis (EMC) virus (17, 18), mengovirus (19, 20), vaccinia virus (21), reovirus (22), West Nile virus (23), and herpes simplex virus type 1 (HSV-1) (24). It also contributes to antibacterial innate immunity and has antiproliferative and apoptotic effector roles (15, 18, 25–28). Its role in the pathogenesis of CS and virus-induced pulmonary responses like COPD, however, has not been investigated.

We hypothesized that RNase L contributes to the inflammatory and remodeling responses induced by viral PAMPs or influenza virus in CS-exposed mice. To test this hypothesis we characterized the 2′-5′OAS/RNase L system in mice exposed to CS and virus/viral PAMPs, alone and in combination, and defined the roles of RNase L in the pathogenesis of the exaggerated inflammatory and remodeling responses in this modeling system. These studies demonstrate that CS interacts in a synergistic manner with viral PAMPs and live influenza virus to induce a number of OAS moieties. They also demonstrate that RNase L plays a critical role in the exaggerated inflammation, fibrosis, emphysema, apoptosis and TGF-β1 and type I IFN production induced by CS and viral PAMPs/virus in combination in the murine lung.

Materials and Methods

Mice

RNase $L^{-/-}$ mice were generated and genotyped as previously described (18). All mice were bred to be congenic on a C57BL/6 background. All animal experiments were approved by

the Yale School of Medicine Institutional Animal Care and Use Committee in accordance with federal guidelines.

Treatment of mice

8 week old WT or RNase $L^{-/-}$ mice were exposed to room air (RA) or the smoke from nonfiltered research cigarettes (2R4; University of Kentucky, Lexington, Kentucky, USA) as previously described by our laboratory (5). During the first week, mice received a half cigarette twice a day to allow for acclimation. During the remainder of the exposure, they received 3 cigarettes per day (1 cigarette/session, 3 sessions/day). Poly(I:C) or influenza A virus were administrated after 2 weeks of CS exposure. Poly(I:C) was used in these experiments to mimic viral double-stranded RNA, which is produced during influenza (or virus) replication. For Poly(I:C) treatment, the mice were anesthetized and 50ng Poly(I:C) or PBS vehicle controls were administered twice per week for 2 weeks via nasal aspiration. CS exposure was continued during this interval. The mice were sacrificed and evaluated 1 day after the last administration. For influenza A treatment, the mice were anesthetized and 5.0 × 103.375 TCID50 (50% tissue culture infective doses) of A/PR8/34 influenza (equivalent to 0.05 LD50 in C57BL/6J mice) was administered via nasal aspiration in 70 μl of PBS. CS exposure was continued during this interval. The mice were sacrificed and evaluated 7 days and 14 days after the virus administration.

Bronchoalveolar lavage (BAL) and histology

Mice were anesthetized, the thorax was opened, right heart perfusion was accomplished with calcium and magnesium-free PBS and BAL was undertaken as previously described (5). Total cell counts were determined using a hemocytometer, and aliquots were cytospun onto microscope slides and stained with Diff-Quick (Dade Behring) for cellular differential assessment. After the BAL, the lungs were removed from the thorax, inflated at 25 cm pressure with PBS containing 0.5% low melting point agarose gel, fixed, embedded in paraffin, sectioned, and stained. Hematoxylin and eosin, and Mallory's trichrome stains were performed in the Research Histology Laboratory of the Department of Pathology at the Yale University School of Medicine.

Quantitative RT-PCR

Total RNA was isolated from whole-lung tissue using Trizol reagent (Invitrogen) and transcript levels were quantified using real-time quantitative RT-PCR. The primer sequences that were employed have been previously described (5).

Immunofluorescence

Lung sections were rehydrated, blocked with 5% BSA, and incubated with rabbit anti-mouse RNase L antibody generated using recombinant mouse RNase L expressed in *E. coli* and purified by FPLC (B.K.J. & R.H.S., to be described elsewhere). The goat anti-mouse SPC antibody was from Santa Cruz (Santa Cruz, CA). Slides were then incubated with anti-goat Alexa Fluor 594and anti-rabbit Alexa Fluor 488 (Invitrogen), then coversliped with Vectashield with DAPI (Vector Laboratories, Burlingame, CA).

Quantification of lung collagen

Animals were anesthetized, right heart perfusion was accomplished with calcium and magnesium-free PBS, the heart and lungs were removed and the right lung was frozen in liquid nitrogen and stored at −80°C until used. Collagen content was determined by quantifying total soluble collagen using the Sircol Collagen Assay kit (Biocolor) according to the manufacturer's instructions. The data is expressed as the collagen content of the entire right lung.

Assessment of alveolar size

Alveolar size was determined in lungs that had been fixed to pressure by measuring mean the chord length of H&E-stained lung sections. Briefly, ten random fields were evaluated by microscopic projection onto the NIH Image program (ver. 1.63), and alveolar size was estimated from the mean chord length of the air space as described previously by our laboratory (5).

TUNEL analysis

End labeling of exposed 3′-OH ends of DNA fragments in paraffin-embedded tissue was undertaken with the TUNEL in situ cell death detection kit AP (Roche Diagnostics). After staining, 8–10 random pictures were obtained from each lung, and a minimum of 300 cells were visually evaluated in each section. The labeled cells were expressed as a percentage of total nuclei.

ELISA

TGF-β1 and IFN-β levels in the mouse BAL samples were quantified in using ELISA kits (R&D Systems for TGF-β1; PBL Biomedical Laboratories for IFN-β) following the manufacturer's instructions.

Statistics

Values are expressed as the mean ± SEM. As appropriate, groups were compared by 2-way ANOVA; follow-up comparisons between groups were conducted using a two-tailed Student t test. A p value of ≤ 0.05 was considered to be significant.

Results

CS interacts with Poly(I:C) or Influenza A to enhance the expression of multiple forms of OAS

In these studies quantitative RT-PCR was performed to define the levels of multiple forms of OAS in lungs from mice treated by nasal aspiration with CS and Poly(I:C) or influenza A, alone and in combination. These evaluations demonstrated that modest levels of mRNA encoding OAS transcripts could be appreciated in lungs from mice in room air (RA) and mice exposed to CS only (Figure 1). Poly(I:C) treatments stimulated the levels of a number of OAS transcripts (Figure 1A–1E). Importantly, many of the OAS transcripts (OAS1D, OAS1G, OAS2, OASL1 and OASL2) were synergistically increased beyond the levels obtained with CS alone and Poly(I:C) alone, in mice exposed to CS and Poly(I:C) in combination (Figure 1A–1E). Other OAS genes, including OAS1A, OAS1B, OAS1C, OAS1E, OAS1H, and OAS3, were not synergistically induced by CS and Poly(I:C) in combination (data not shown). To begin to understand the effects of CS plus live virus, mice were exposed to RA or CS for 2 weeks, infected with influenza A and qRT-PCR was used to quantitate the levels of multiple forms of OAS. These studies demonstrated that CS and live virus, individually, did not alter levels of OAS2 and OAS3 transcripts and only modestly increased levels of OASL1 transcripts (Figure 1F–1H). In contrast, CS exposure and virus infection interacted to synergistically increase the expression of these OAS moieties (Figure 1F–1H). Other forms of OAS genes, including genes in the OAS1 family and OASL2, were not synergistically induced by CS and influenza A (data not shown). These studies demonstrate that CS and Poly(I:C) or influenza A interact to synergistically stimulate multiple forms of OAS in the murine lung.

RNase L is expressed in type II alveolar epithelial cells in the lungs from mice treated with CS plus Poly(I:C) or influenza A

Because OAS moieties are important activators of RNase L, immunofluorescent studies were next undertaken to localize RNase L in lungs from mice treated with CS and Poly(I:C) or influenza A, alone and in combination. These evaluations demonstrated that weak RNase L staining could be appreciated in lungs from mice in room air (RA) and mice exposed to CS only (Figure 2). Poly(I:C) or influenza A treatments stimulated the expression of RNase L (Figure 2). Importantly, the levels of RNase L expression in lungs from mice exposed to CS plus Poly(I:C) or influenza A in combination were greater than the levels in mice treated with each moiety individually (Figure 2). This RNase L expression co-localized with the type II alveolar epithelial cell marker Surfactant apoprotein C (SPC) (Figure 2, white arrows). Thus, these studies demonstrate that CS and Poly(I:C) or influenza A interact to synergistically stimulate RNase L expression in type II alveolar epithelial cells in the murine lung.

The exaggerated inflammation induced by CS and Poly(I:C) or influenza A virus in combination is decreased in the absence of RNase L

As previously reported by our laboratory (5), CS exposure caused a mild increase in bronchoalveolar lavage (BAL) total cell recovery, Poly(I:C) significantly increased total cell, macrophage, lymphocyte, and neutrophil recovery and CS and Poly(I:C) interacted in a synergistic manner to enhance these inflammatory responses (Figure 3A). To evaluate the importance of RNase L in these responses we compared the effects of these interventions in wild type (WT) and RNase $L^{-/-}$ animals. These studies demonstrated that the inflammatory effects of CS or Poly(I:C) individually were not significantly altered in the absence of RNase L. In contrast, the synergistic interactions of Poly(I:C) treatment and CS exposure were significantly diminished in animals with null mutations of RNase L (Figure 3A and B). This manifest as a significant decrease in total inflammatory cell and macrophage, lymphocyte and neutrophil recovery in the BAL fluids from RNase $L^{-/-}$ mice compared to WT controls (Figure 3A and B). These data demonstrate that exaggerated pulmonary inflammatory response induced by CS and Poly(I:C) in combination is significantly diminished in the lungs of RNase $L^{-/-}$ mice compared to WT controls.

To define the role(s) of RNase L in the pulmonary inflammation induced by CS plus influenza A, WT and RNase $L^{-/-}$ mice were exposed to RA or CS followed by influenza A infection. BAL inflammation was evaluated 7 days after viral inoculation. Virus infection caused significant increases in total cell (Figure 3C), and macrophage, lymphocyte, and neutrophil recovery that peaked 7 days after viral inoculation (Figure 3D). Interestingly, CS and influenza A also interacted in a synergistic manner to enhance this inflammatory response (Figure 3C and D). The stimulatory effects of influenza were not significantly altered in the absence of RNase L (Figure 3C and D). In contrast, the augmented inflammation induced by CS and virus in combination was markedly decreased in RNase L null mice (Figure 3C and D). There was a significant decrease in total BAL cell recovery and neutrophil, macrophage and lymphocyte recovery in RNase L null mice versus WT controls (Figure 3C and D). Together, these studies demonstrate that the heightened pulmonary inflammatory response induced by CS plus virus is mediated by an RNase L-dependent mechanism(s).

RNase L plays a critical role in the airway fibrosis induced by CS plus Poly (I:C) or influenza A

As previously reported by our laboratory (5), CS and Poly(I:C) individually did not induce collagen deposition while airway fibrosis was a prominent feature in the lungs of mice that are exposed to CS and Poly(I:C) in combination (Figure 4A and B). To define the role(s) of

RNase L in these remodeling responses we compared the fibrosis in WT and RNase L null mice treated with CS and Poly(I:C), alone and in combination. As shown in Figure 4, trichrome histologic evaluations and sircol collagen assays demonstrated that the fibrosis and collagen accumulation in mice treated with CS or Poly(I:C) individually were not altered in the absence of RNase L. In contrast, the fibrosis and collagen accumulation in mice treated with CS plus Poly(I:C) were significantly decreased in lungs from RNase L null mice compared to similarly treated WT controls. In accord with these findings, the levels of BAL total TGF-β1 were significantly increased in WT mice treated with CS and Poly(I:C) in combination and these inductive effects were significantly ameliorated in the absence of RNase L (Figure 4C). Similarly, virus infection caused a modest increase in collagen accumulation that peaked 14 days after viral inoculation (Figure 5A and B). This response was further augmented in mice treated with CS and influenza in combination (Figure 5A and B). The fibrotic response induced by influenza alone was not significantly altered in the absence of RNase L (Figure 5A and B). In contrast, 14 days after viral inoculation, the augmented response induced by CS and virus in combination was significantly decreased in the absence of RNase L (Figure 5A and B). In accord with these findings, the levels of BAL total TGF-β1 were modestly increased in mice infected with influenza alone and synergistically increased in mice exposed to CS plus influenza (Figure 5C). The levels of total TGF-β1 were decreased in mice infected with influenza A alone but these changes did not reach statistical significance (Figure 5C). In contrast, the induction in mice exposed to CS and virus was significantly decreased in the absence of RNase L (Figure 5C). When viewed in combination, these data demonstrate that the fibrotic tissue remodeling and TGF-β1 induced by CS plus Poly(I:C) or influenza A in combination are significantly diminished in the lungs from RNase $L^{-/-}$ mice compared with WT controls.

RNase L plays a critical role in the airspace destruction induced by CS plus Poly(I:C) or influenza A

As previously reported (5), CS and Poly(I:C) or virus individually did not induce significant alveolar remodeling while alveolar remodeling and enlargement were readily appreciated in the lungs of mice that were exposed to CS plus Poly(I:C) or influenza A in combination (Figure 6 and 7). To define the role(s) of RNase L in these alveolar remodeling responses we compared the alveoli in WT and RNase L null mice treated with CS and Poly(I:C) or influenza A, alone and in combination. As shown in Figure 6, treatment with CS or Poly(I:C) individually did not cause significant alveolar enlargement in the presence or absence of RNase L. In contrast, alveolar chord length measurements were significantly increased in lungs from mice exposed to CS plus Poly(I:C) (Figure 6A and B). Importantly, this alveolar remodeling was significantly ameliorated in the absence of RNase L (Figure 6A and B). Treatment with CS and Poly(I:C) in combination also caused significant alveolar injury with alveolar epithelial DNA injury/apoptosis on TUNEL evaluations (Figure 6C). This injury/cell death response was also significantly decreased in mice that lacked RNase L (Figure 6C). In the settings of live virus infection, alveolar remodeling peaked 14 days after viral inoculation. Similar to Poly(I:C) treatment, the effects of CS and virus individually were not significantly altered in the absence of RNase L (Figure 7A and B). In contrast, the heightened alveolar remodeling in mice exposed to CS and virus, in combination, was markedly decreased in RNase L null animals (Figure 7A and B). In accord with these findings, CS and virus individually did not alter or only modestly increased the number of TUNEL positive alveolar epithelial cells while CS exposure plus virus significantly increase the number of TUNEL positive cells in these animals (Figure 7C). Importantly, this augmented DNA injury/cell death response was markedly diminished in mice that lack RNase L (Figure 7C). Together, these findings demonstrate that the alveolar remodeling and epithelial apoptosis in lungs from mice treated with CS plus Poly(I:C) or influenza A are mediated via an RNase L-dependent mechanism(s).

RNase L plays a critical role in the stimulation of Type I IFN by CS plus Poly(I:C) or influenza A

Studies were next undertaken to define the role(s) of RNase L in the stimulation of type I IFNs in the lung. As previously described (5), CS did not cause major alterations, Poly(I:C) stimulated and CS plus Poly(I:C) interacted to further increase type I IFN mRNA and protein accumulation (Figure 8). The effects of CS and Poly(I:C) individually were not altered in the absence of RNase L (Figure 8A–C). In contrast, the augmented stimulation of type I IFN by CS plus Poly(I:C) was markedly decreased in RNase $L^{-/-}$ mice(Figure 8A–C). In the settings of live virus infection, influenza A infection resulted in Type I IFN production that peaked on Day 7 and diminished thereafter. This Type I IFN was significantly augmented in mice exposed to CS (Data not shown). Interestingly, after treatment with CS plus virus, null mutations of RNase L resulted in defective viral resistance and titers of virus that were approximately 4-fold higher in RNase L null versus WT mice at Day 7 after viral inoculation (Supplemental Figure S1A). Despite this increase in virus accumulation, the production of Type I IFN was comparable or only slightly increased in RNase $L^{-/-}$ mice (Supplemental Figure S1B–D). To obtain an index of the ability of the lungs from WT and RNase L null mice to produce Type I IFN when infected we looked at the relationship between the levels of Type I IFN and viral load. As can be seen in Figure 8 in panels D–F, when the levels of Type I IFN were normalized to viral titer, it is clear that lungs from RNase L null mice have a decreased ability to produce Type I IFNs compared to infected WT controls. In combination, these studies demonstrate that RNase L plays a critical role in Type I IFN production induced by CS plus Poly(I:C) or influenza A.

Discussion

Clinical observations suggest that interactions between CS exposure and viral infection play important roles in the pathogenesis of a variety of diseases including COPD, the enhanced morbidity in respiratory syncytial virus (RSV)-infected, second hand smoke-exposed children and the enhanced mortality in virus-infected otherwise normal smokers (9, 10, 29–34). In many of these settings virus infection/exposure is believed to result in inflammatory responses that overwhelm protective anti-inflammatory defenses (6, 35). In keeping with these clinical observations studies from our laboratory and others have demonstrated that CS selectively enhances the airway and parenchymal inflammatory, remodeling, and apoptotic responses induced by viral PAMPs and demonstrated the importance of a type I IFN-IL-18-IL-12/IL-23 p40-IFN-γ cytokine cascade, the activation of PKR (double stranded RNA-dependent protein kinase) and eIF2α and MAVS in these events (5). The present studies add to these observations by testing the hypothesis that the 2′-5′OAS/RNase L pathway also contributes to these augmented responses. These studies demonstrate that CS and viral PAMPs/live virus interact in a synergistic manner to stimulate OAS moieties. They also demonstrate that RNase L plays a critical role in the pathogenesis of the exaggerated inflammatory, fibrotic, emphysematous, apoptotic and cytokine responses induced by CS and virus/viral PAMPs in combination.

The 2′-5′ OAS/RNase L system was one of the first antiviral pathways discovered during investigations on how IFN inhibits viral infection (15). IFNs induce OAS genes in higher vertebrates and OAS proteins are pathogen recognition receptors (PRR) for viral PAMPs which use ATP to synthesize 2′-5′ linked oligoadenylates that activate RNase L(15). Regulated turnover and processing of RNA by RNase L is essential for the complete IFN response against some viral infections. Activated RNase L also has pro-apoptotic and growth inhibitory properties (15). Our studies add to these observations a number of novel ways. First, they demonstrate that CS is an important regulator of viral/viral PAMP activation of OAS moieties and RNase L. They also demonstrate that this pathway is impressively activated in lungs from mice exposed to CS and virus/viral PAMP in

combination compared to mice exposed to either individually. In keeping with the importance of IFNs in the pathogenesis of the inflammatory and remodeling responses induced by CS and virus/PAMP in combination (5), they also implicate the 2′-5′OAS/RNase L pathway in the pathogenesis of COPD and emphysematous and fibrotic tissue remodeling.

Four classes of OAS genes (OAS1, OAS2, OAS3, and OAS-like) have been identified in the human and mouse OAS gene family (36–38). There are at least 8 different isoforms of OAS1, in addition to OAS2, OAS3, and two isoforms of OAS-like proteins in the mouse (36). These proteins are expressed in a cell/tissue specific manner, display differences in levels of dsRNA required for optimal activation, and have distinct roles in the responses against specific viruses by synthesizing 2–5A of different lengths (19, 39–41). Our studies demonstrate that all OAS subtypes are expressed in the lung. They also demonstrate that these moieties are differentially regulated by synthetic dsRNA and live virus. Specifically, only two isoforms of OAS1 were synergistically induced by CS and Poly(I:C) in combination, while only OAS2 and OASL1 proteins were induced by live influenza virus. The mechanisms of the stimulus- and isoform-specific effects and their importance in CS plus viral PAMP/virus-induced inflammatory, apoptotic, destructive, fibrotic and cytokine responses in the lung will need additional investigation.

The emphysematous alveolar destruction that is characteristic of COPD has been attributed to a variety of abnormalities including protease excess and oxidant injury (42, 43). Recently, the apoptosis of endothelial and epithelial cells has been proposed to be a critical event in the genesis of these abnormalities (44). In keeping with the importance of this cell death response we previously noted that the alveolar destruction that is induced by CS plus viral PAMPs/live virus are associated with exaggerated epithelial TUNEL responses (5). Our studies add to these findings by demonstrating that RNase L is expressed in type II alveolar epithelial cells and plays a critical role in this cell death response. Although the mechanism of this contribution is not clear, it is important to point out that, in addition to viral RNA, RNase L can also target cellular RNAs. These targets include ribosome RNA and mitochondrial mRNA and can engender apoptosis of infected cells (25, 26, 28, 45–47). Thus, one can easily see how the sustained activation of RNase L in mice exposed to CS plus Poly(I:C)/flu virus can trigger apoptotic alveolar destruction.

Excessive extracellular matrix accumulation and fibrotic remodeling are common consequences of antipathogen immune responses (48, 49). In some cases they are protective and serve to wall the pathogen off or induce tissue repair. In others the fibrotic response itself causes tissue dysfunction and has adverse consequences. Airway fibrosis is well documented in COPD and has been proposed to contribute to the airflow obstruction that these patient experience (50). Our studies provide interesting insights into the fibrosis in COPD and possibly other disorders. Specifically, they demonstrate that RNase L plays a critical role(s) in the fibrosis that is induced by CS plus viral PAMPs in combination. They also provide a potential mechanism for this finding by demonstrating that RNase L also plays an important role in the stimulation of TGF-β1. To our knowledge, this is the first demonstration that RNase L can play a role in the pathogenesis of tissue fibrosis or the regulation of TGF-β1. These observations raise the interesting possibility that viruses, viral PAMPs and or the 2′-5′ OAS/RNase L system may play similarly important roles in the pathogenesis of other idiopathic fibrotic disorders such as idiopathic pulmonary fibrosis or scleroderma.

As noted above, RNase L is indirectly activated by IFN in combination with viral dsRNA. Interestingly, our studies also demonstrate that the induction of type I IFNs by CS plus viral PAMPs is decreased in the absence of RNase L. These findings may be explained by the

ability of RNase L to generate small RNAs which activate the RIG-Iike helicase (RLH) pathway and induce the transcription of Type I IFN genes (51). Regardless, one can envision a positive feedback loop here where viral infection/exposure induces type l IFN in CS-exposed tissues (via the RLH or the 2′-5′OAS/RNase L pathways) which further activates RNase L and increases IFN elaboration. One can envision how this sort of a positive feedback loop could contribute to the chronicity and or intensity of CS plus virus-induced responses.

To thoroughly understand the interactions of CS exposure and viral infection we used viral PAMPs and live virus. This comparison was undertaken to avoid the confounding effects that could be seen with altered titers of live virus in RNase L null mice. Our studies with Poly(I:C) clearly demonstrate that the induction of Type l IFNs in CS-exposed mice was decreased in the absence of RNase L. Similar results were not noted with live virus. In these experiments the titers of Influenza in RNase L null mice were significantly higher than in WT controls. Importantly, when the increased titers of influenza in CS-exposed RNase L null mice were taken into account it is clear that CS-exposed RNase L deficient mice also have a defect in Type l IFN elaboration. It is also important to point out that, despite the increased titers of virus in the CS-exposed RNase L null mice, virus induced phenotypes were ameliorated in lungs from these animals. These findings reinforce the importance of RNase L in mediating the tissue effects of virus in smoke-exposed tissues.

Influenza virus non-structural protein 1 (NS1) has the ability to bind dsRNA and sequester the activation of OAS thereby counteracting the anti-viral responses induced by the IFN-OAS-RNase L system (52). This viral evasion mechanism is utilized by influenza A virus and numerous studies have demonstrated that RNase L has no effect on viral replication in cells infected with flu virus (52). In accord with these observations, we noted that when mice were treated with Poly(I:C) or virus alone, null mutations of RNase L did not alter inflammatory or tissue destructive responses and significant difference in pulmonary pathology were not observed in comparisons of lungs from RNase $L^{-/-}$ and WT mice. However, when mice were exposed with CS before inoculation with Influenza, RNase L exhibited impressive antiviral effects and diminished inflammatory and tissue remodeling responses. These observations suggest that CS alters the NS1-based evasion mechanism that is operative in room air exposed mice and enhances the importance of RNase L in viral control and clearance.

In conclusion, our studies demonstrate that the 2′-5′ OAS/RNase L system is activated in lungs from mice exposed to CS plus viral PAMPs/live virus. They also demonstrate that RNase L plays a critical role in the pathogenesis of the exaggerated inflammatory, emphysematous, fibrotic, apoptotic and cytokine responses that are induced by CS and virus/PAMP in combination. These finding suggest that this activation plays an important role in the pathogenesis of COPD and other diseases in which interactions between CS exposure and viral infection play an important pathogenetic role. They also suggest that polymorphisms in the 2′-5′OAS/RNase L system might be able to contribute to the susceptibility and heterogeneity of these disorders (53, 54). If the anti-inflammatory, remodeling controlling and antiviral properties of RNase L can be appropriately balanced, RNase L may be an important therapeutic target in COPD and other disorders. This is an exciting prospect because naturally occurring RNase L inhibitors have been described (55, 56). Additional investigation of RNase L in health and disease is warranted.

Supplementary Material

Refer to Web version on PubMed Central for supplementary material.

Acknowledgments

This work was supported in part by National Institutes of Health (NIH) grant R01 HL-079328 and Flight Attendant Medical Research Institute grant 82571 (to J.A.E.) and by NIH grant R01 CA-044059 (to R.H.S.).

Abbreviations used in this paper

CS	cigarette smoke
COPD	chronic obstructive pulmonary disease
OAS	oligoadenylatesynthetase
PAMPs	pattern associated molecular patterns
IFN	interferon
MAVS	mitochondrial antiviral signaling molecule
RNase L	Ribonuclease L
EMC	encephalomyocarditis
HSV-1	simplex virus type 1
BAL	Bronchoalveolar lavage
RSV	respiratory syncytial virus
PRR	pathogen recognition receptor
NS-1	non-structural protein 1

References

1. Sutherland ER, Cherniack RM. Management of chronic obstructive pulmonary disease. The New England journal of medicine. 2004; 350:2689–2697. [PubMed: 15215485]
2. Hogg JC, Chu F, Utokaparch S, Woods R, Elliott WM, Buzatu L, Cherniack RM, Rogers RM, Sciurba FC, Coxson HO, Pare PD. The nature of small-airway obstruction in chronic obstructive pulmonary disease. The New England journal of medicine. 2004; 350:2645–2653. [PubMed: 15215480]
3. Sutherland ER. Outpatient treatment of chronic obstructive pulmonary disease: comparisons with asthma. J Allergy Clin Immunol. 2004; 114:715–724. quiz 725. [PubMed: 15480305]
4. Traves SL, Proud D. Viral-associated exacerbations of asthma and COPD. Curr Opin Pharmacol. 2007; 7:252–258. [PubMed: 17369093]
5. Kang MJ, Lee CG, Lee JY, Dela Cruz CS, Chen ZJ, Enelow R, Elias JA. Cigarette smoke selectively enhances viral PAMP- and virus-induced pulmonary innate immune and remodeling responses in mice. The Journal of clinical investigation. 2008; 118:2771–2784. [PubMed: 18654661]
6. Sapey E, Stockley RA. COPD exacerbations. 2: aetiology. Thorax. 2006; 61:250–258. [PubMed: 16517585]
7. Ball P. Epidemiology and treatment of chronic bronchitis and its exacerbations. Chest. 1995; 108:43S–52S. [PubMed: 7634925]
8. Mallia P, Johnston SL. How viral infections cause exacerbation of airway diseases. Chest. 2006; 130:1203–1210. [PubMed: 17035457]
9. Seemungal T, Harper-Owen R, Bhowmik A, Moric I, Sanderson G, Message S, Maccallum P, Meade TW, Jeffries DJ, Johnston SL, Wedzicha JA. Respiratory viruses, symptoms, and inflammatory markers in acute exacerbations and stable chronic obstructive pulmonary disease. American journal of respiratory and critical care medicine. 2001; 164:1618–1623. [PubMed: 11719299]

10. Wedzicha JA. Role of viruses in exacerbations of chronic obstructive pulmonary disease. Proceedings of the American Thoracic Society. 2004; 1:115–120. [PubMed: 16113423]
11. Bals R, Hiemstra PS. Innate immunity in the lung: how epithelial cells fight against respiratory pathogens. Eur Respir J. 2004; 23:327–333. [PubMed: 14979512]
12. Robbins CS, Bauer CM, Vujicic N, Gaschler GJ, Lichty BD, Brown EG, Stampfli MR. Cigarette smoke impacts immune inflammatory responses to influenza in mice. American journal of respiratory and critical care medicine. 2006; 174:1342–1351. [PubMed: 17023734]
13. Motz GT, Eppert BL, Wortham BW, Amos-Kroohs RM, Flury JL, Wesselkamper SC, Borchers MT. Chronic cigarette smoke exposure primes NK cell activation in a mouse model of chronic obstructive pulmonary disease. Journal of immunology. 2010; 184:4460–4469.
14. Wortham BW, Eppert BL, Motz GT, Flury JL, Orozco-Levi M, Hoebe K, Panos RJ, Maxfield M, Glasser SW, Senft AP, Raulet DH, Borchers MT. NKG2D mediates NK cell hyperresponsiveness and influenza-induced pathologies in a mouse model of chronic obstructive pulmonary disease. Journal of immunology. 2012; 188:4468–4475.
15. Chakrabarti A, Jha BK, Silverman RH. New insights into the role of RNase L in innate immunity. J Interferon Cytokine Res. 2010; 31:49–57. [PubMed: 21190483]
16. Bisbal C, Silverman RH. Diverse functions of RNase L and implications in pathology. Biochimie. 2007; 89:789–798. [PubMed: 17400356]
17. Williams BR, Golgher RR, Brown RE, Gilbert CS, Kerr IM. Natural occurrence of 2–5A in interferon-treated EMC virus-infected L cells. Nature. 1979; 282:582–586. [PubMed: 95208]
18. Zhou A, Paranjape J, Brown TL, Nie H, Naik S, Dong B, Chang A, Trapp B, Fairchild R, Colmenares C, Silverman RH. Interferon action and apoptosis are defective in mice devoid of 2′, 5′-oligoadenylate-dependent RNase L. EMBO J. 1997; 16:6355–6363. [PubMed: 9351818]
19. Chebath J, Benech P, Revel M, Vigneron M. Constitutive expression of (2′-5′) oligo A synthetase confers resistance to picornavirus infection. Nature. 1987; 330:587–588. [PubMed: 2825034]
20. Rysiecki G, Gewert DR, Williams BR. Constitutive expression of a 2′,5′-oligoadenylate synthetase cDNA results in increased antiviral activity and growth suppression. J Interferon Res. 1989; 9:649–657. [PubMed: 2481699]
21. Rice AP, Roberts WK, Kerr IM. 2–5A accumulates to high levels in interferon-treated, vaccinia virus-infected cells in the absence of any inhibition of virus replication. J Virol. 1984; 50:220–228. [PubMed: 6422053]
22. Nilsen TW, Maroney PA, Baglioni C. Synthesis of (2′-5′)oligoadenylate and activation of an endoribonuclease in interferon-treated HeLa cells infected with reovirus. J Virol. 1982; 42:1039–1045. [PubMed: 6178844]
23. Scherbik SV, Paranjape JM, Stockman BM, Silverman RH, Brinton MA. RNase L plays a role in the antiviral response to West Nile virus. J Virol. 2006; 80:2987–2999. [PubMed: 16501108]
24. Austin BA, James C, Silverman RH, Carr DJ. Critical role for the oligoadenylate synthetase/RNase L pathway in response to IFN-beta during acute ocular herpes simplex virus type 1 infection. Journal of immunology. 2005; 175:1100–1106.
25. Wreschner DH, James TC, Silverman RH, Kerr IM. Ribosomal RNA cleavage, nuclease activation and 2–5A(ppp(A2′p)nA) in interferon-treated cells. Nucleic Acids Res. 1981; 9:1571–1581. [PubMed: 6164990]
26. Silverman RH, Skehel JJ, James TC, Wreschner DH, Kerr IM. rRNA cleavage as an index of ppp(A2′p)nA activity in interferon-treated encephalomyocarditis virus-infected cells. J Virol. 1983; 46:1051–1055. [PubMed: 6190010]
27. Castelli JC, Hassel BA, Wood KA, Li XL, Amemiya K, Dalakas MC, Torrence PF, Youle RJ. A study of the interferon antiviral mechanism: apoptosis activation by the 2–5A system. J Exp Med. 1997; 186:967–972. [PubMed: 9294150]
28. Rusch L, Zhou A, Silverman RH. Caspase-dependent apoptosis by 2′,5′-oligoadenylate activation of RNase L is enhanced by IFN-beta. J Interferon Cytokine Res. 2000; 20:1091–1100. [PubMed: 11152576]
29. Bhowmik A, Seemungal TA, Sapsford RJ, Wedzicha JA. Relation of sputum inflammatory markers to symptoms and lung function changes in COPD exacerbations. Thorax. 2000; 55:114–120. [PubMed: 10639527]

30. Tan WC, Xiang X, Qiu D, Ng TP, Lam SF, Hegele RG. Epidemiology of respiratory viruses in patients hospitalized with near-fatal asthma, acute exacerbations of asthma, or chronic obstructive pulmonary disease. Am J Med. 2003; 115:272–277. [PubMed: 12967691]
31. Arcavi L, Benowitz NL. Cigarette smoking and infection. Arch Intern Med. 2004; 164:2206–2216. [PubMed: 15534156]
32. Cohen S, Tyrrell DA, Russell MA, Jarvis MJ, Smith AP. Smoking, alcohol consumption, and susceptibility to the common cold. Am J Public Health. 1993; 83:1277–1283. [PubMed: 8363004]
33. Kark JD, Lebiush M. Smoking and epidemic influenza-like illness in female military recruits: a brief survey. Am J Public Health. 1981; 71:530–532. [PubMed: 7212144]
34. Kark JD, Lebiush M, Rannon L. Cigarette smoking as a risk factor for epidemic a(h1n1) influenza in young men. The New England journal of medicine. 1982; 307:1042–1046. [PubMed: 7121513]
35. Papi A, Bellettato CM, Braccioni F, Romagnoli M, Casolari P, Caramori G, Fabbri LM, Johnston SL. Infections and airway inflammation in chronic obstructive pulmonary disease severe exacerbations. American journal of respiratory and critical care medicine. 2006; 173:1114–1121. [PubMed: 16484677]
36. Kakuta S, Shibata S, Iwakura Y. Genomic structure of the mouse 2′,5′-oligoadenylate synthetase gene family. J Interferon Cytokine Res. 2002; 22:981–993. [PubMed: 12396720]
37. Kristiansen H, Gad HH, Eskildsen-Larsen S, Despres P, Hartmann R. The oligoadenylate synthetase family: an ancient protein family with multiple antiviral activities. J Interferon Cytokine Res. 2010; 31:41–47. [PubMed: 21142819]
38. Silverman RH. Viral encounters with 2′,5′-oligoadenylate synthetase and RNase L during the interferon antiviral response. J Virol. 2007; 81:12720–12729. [PubMed: 17804500]
39. Chebath J, Benech P, Hovanessian A, Galabru J, Revel M. Four different forms of interferon-induced 2′,5′-oligo(A) synthetase identified by immunoblotting in human cells. J Biol Chem. 1987; 262:3852–3857. [PubMed: 2434505]
40. Hovanessian AG, Svab J, Marie I, Robert N, Chamaret S, Laurent AG. Characterization of 69- and 100-kDa forms of 2–5A-synthetase from interferon-treated human cells. J Biol Chem. 1988; 263:4945–4949. [PubMed: 3350819]
41. Lin RJ, Yu HP, Chang BL, Tang WC, Liao CL, Lin YL. Distinct antiviral roles for human 2′,5′-oligoadenylate synthetase family members against dengue virus infection. Journal of immunology. 2009; 183:8035–8043.
42. Abboud RT, Vimalanathan S. Pathogenesis of COPD. Part I. The role of protease-antiprotease imbalance in emphysema. Int J Tuberc Lung Dis. 2008; 12:361–367. [PubMed: 18371259]
43. MacNee W. Oxidants/antioxidants and COPD. Chest. 2000; 117:303S–317S. [PubMed: 10843965]
44. Demedts IK, Demoor T, Bracke KR, Joos GF, Brusselle GG. Role of apoptosis in the pathogenesis of COPD and pulmonary emphysema. Respir Res. 2006; 7:53. [PubMed: 16571143]
45. Lewis JA, Huq A, Najarro P. Inhibition of mitochondrial function by interferon. J Biol Chem. 1996; 271:13184–13190. [PubMed: 8662694]
46. Bernardi P, Scorrano L, Colonna R, Petronilli V, Di Lisa F. Mitochondria and cell death. Mechanistic aspects and methodological issues. Eur J Biochem. 1999; 264:687–701. [PubMed: 10491114]
47. Zhou A, Paranjape JM, Hassel BA, Nie H, Shah S, Galinski B, Silverman RH. Impact of RNase L overexpression on viral and cellular growth and death. J Interferon Cytokine Res. 1998; 18:953–961. [PubMed: 9858317]
48. Qiao J, Zhang M, Bi J, Wang X, Deng G, He G, Luan Z, Lv N, Xu T, Zhao L. Pulmonary fibrosis induced by H5N1 viral infection in mice. Respir Res. 2009; 10:107. [PubMed: 19909524]
49. Mora AL, Woods CR, Garcia A, Xu J, Rojas M, Speck SH, Roman J, Brigham KL, Stecenko AA. Lung infection with gamma-herpesvirus induces progressive pulmonary fibrosis in Th2-biased mice. Am J Physiol Lung Cell Mol Physiol. 2005; 289:L711–721. [PubMed: 15734789]
50. Barnes PJ. Small airways in COPD. The New England journal of medicine. 2004; 350:2635–2637. [PubMed: 15215476]
51. Malathi K, Dong B, Gale M Jr, Silverman RH. Small self-RNA generated by RNase L amplifies antiviral innate immunity. Nature. 2007; 448:816–819. [PubMed: 17653195]

52. Min JY, Krug RM. The primary function of RNA binding by the influenza A virus NS1 protein in infected cells: Inhibiting the 2′-5′ oligo (A) synthetase/RNase L pathway. Proc Natl Acad Sci U S A. 2006; 103:7100–7105. [PubMed: 16627618]

53. Yakub I, Lillibridge KM, Moran A, Gonzalez OY, Belmont J, Gibbs RA, Tweardy DJ. Single nucleotide polymorphisms in genes for 2′-5′-oligoadenylate synthetase and RNase L inpatients hospitalized with West Nile virus infection. The Journal of infectious diseases. 2005; 192:1741–1748. [PubMed: 16235172]

54. Field LL, Bonnevie-Nielsen V, Pociot F, Lu S, Nielsen TB, Beck-Nielsen H. OAS1 splice site polymorphism controlling antiviral enzyme activity influences susceptibility to type 1 diabetes. Diabetes. 2005; 54:1588–1591. [PubMed: 15855350]

55. Bisbal C, Martinand C, Silhol M, Lebleu B, Salehzada T. Cloning and characterization of a RNAse L inhibitor. A new component of the interferon-regulated 2–5A pathway. J Biol Chem. 1995; 270:13308–13317. [PubMed: 7539425]

56. Le Roy F, Bisbal C, Silhol M, Martinand C, Lebleu B, Salehzada T. The 2–5A/RNase L/RNase L inhibitor (RLI) [correction of (RNI)] pathway regulates mitochondrial mRNAs stability in interferon alpha-treated H9 cells. J Biol Chem. 2001; 276:48473–48482. [PubMed: 11585831]

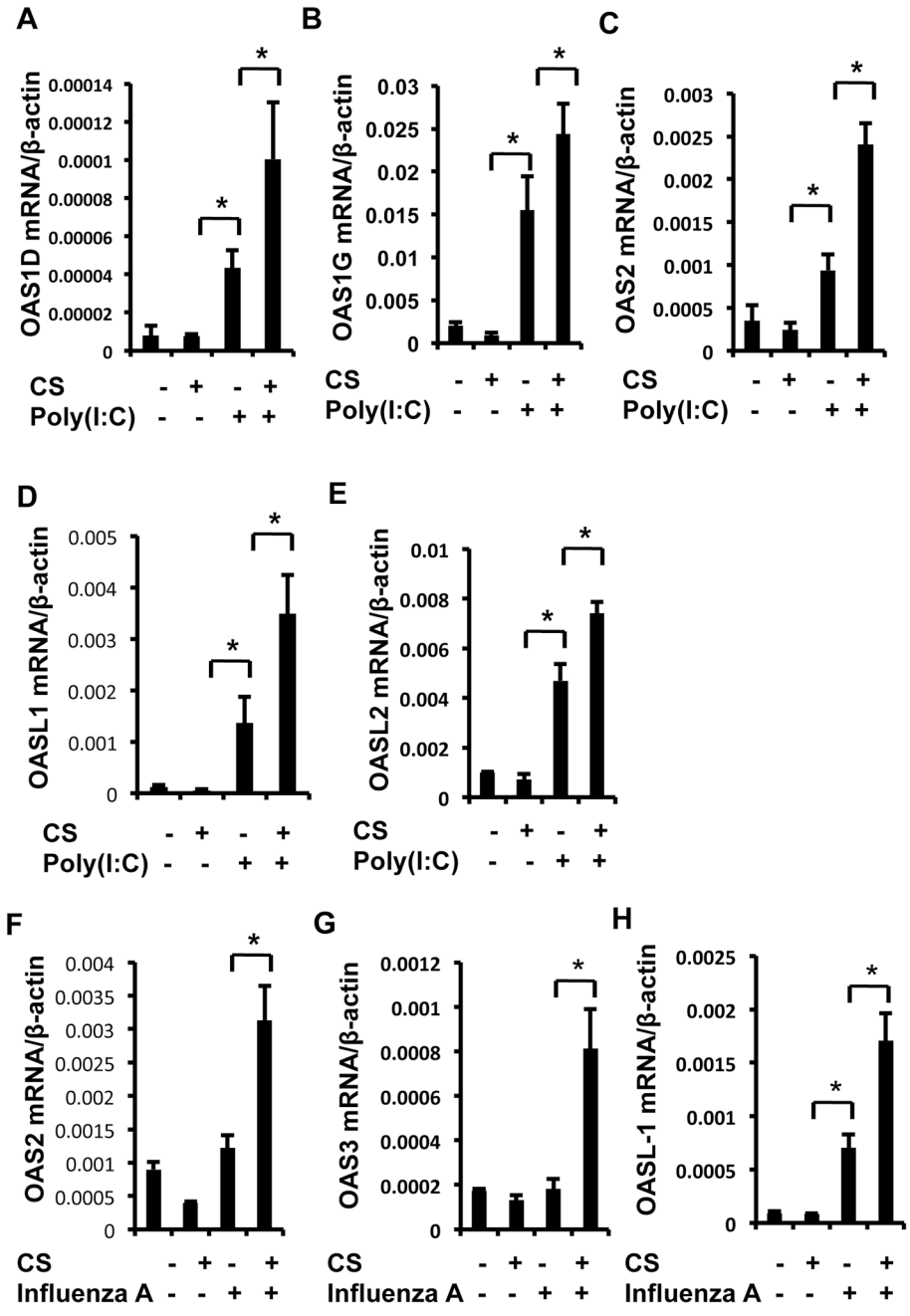

FIGURE 1.

OAS gene expression in the lungs from mice treated with CS plus Poly(I:C) or influenza A, alone or in combination. The levels of mRNA encoding various forms of OAS were measured in whole-lung RNA extracts using quantitative RT-PCR. (A) OAS1D; (B) OAS1G; (C) OAS2; (D) OASL1; (E) OASL2; (F) OAS2; (G) OAS3; (H) OASL1. The data are presented as the mean +/− SEM percentage of concurrent β-actin evaluations. n = 4 for each. *, P≤0.05.

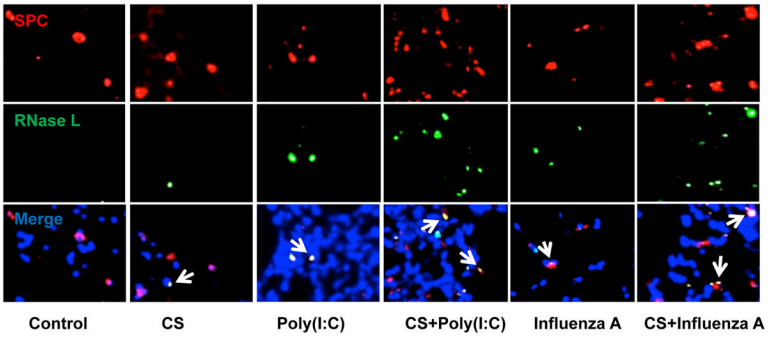

FIGURE 2.

Localization of RNase L in the lungs from mice treated with CS plus Poly(I:C) or influenza A, alone or in combination. Type II epithelial cells were stained with an anti-SPC antibody and then labeled with red fluorescence (alexafluor 594). RNase L was labeled with green fluorescence (alexafluor 488). Nuclei are stained with DAPI (blue). Sites of co-localization of RNase L and SPC are highlighted with white arrows.

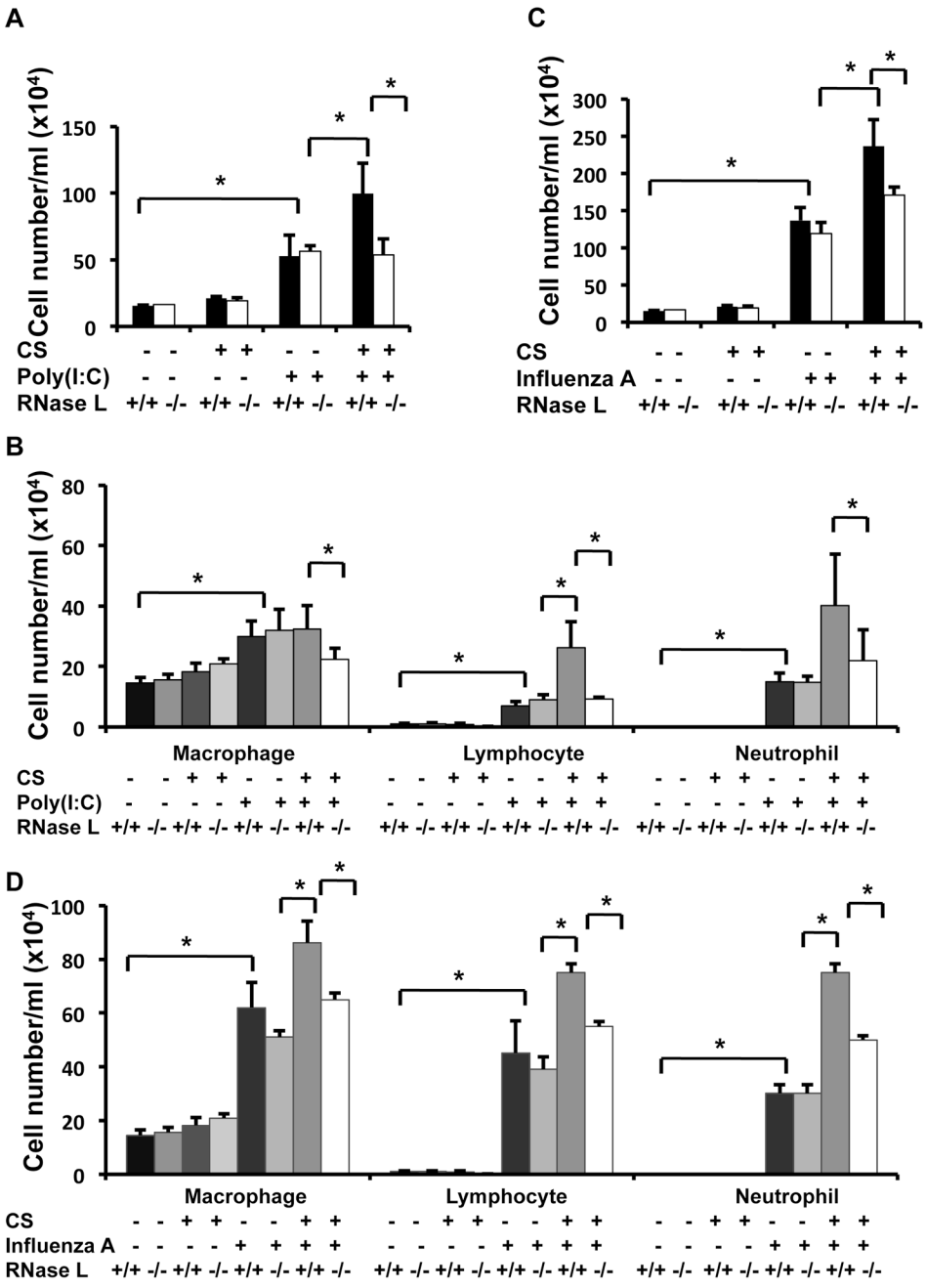

FIGURE 3.

Role of RNase L in the pulmonary inflammation in lungs from mice exposed to CS plus Poly(I:C) or influenza A, alone and in combination. WT or RNase $L^{-/-}$ mice were exposed to CS(+) or room air (CS−) and randomized to receive Poly(I:C), Influenza A virus or vehicle. In (A) and (C), BAL fluid was collected, and total cell recovery was determined. In (B) and (D), BAL cell differential was assessed. The noted values represent the mean +/− SEM of evaluations in a minimum of 4 mice; * $P \leq 0.05$

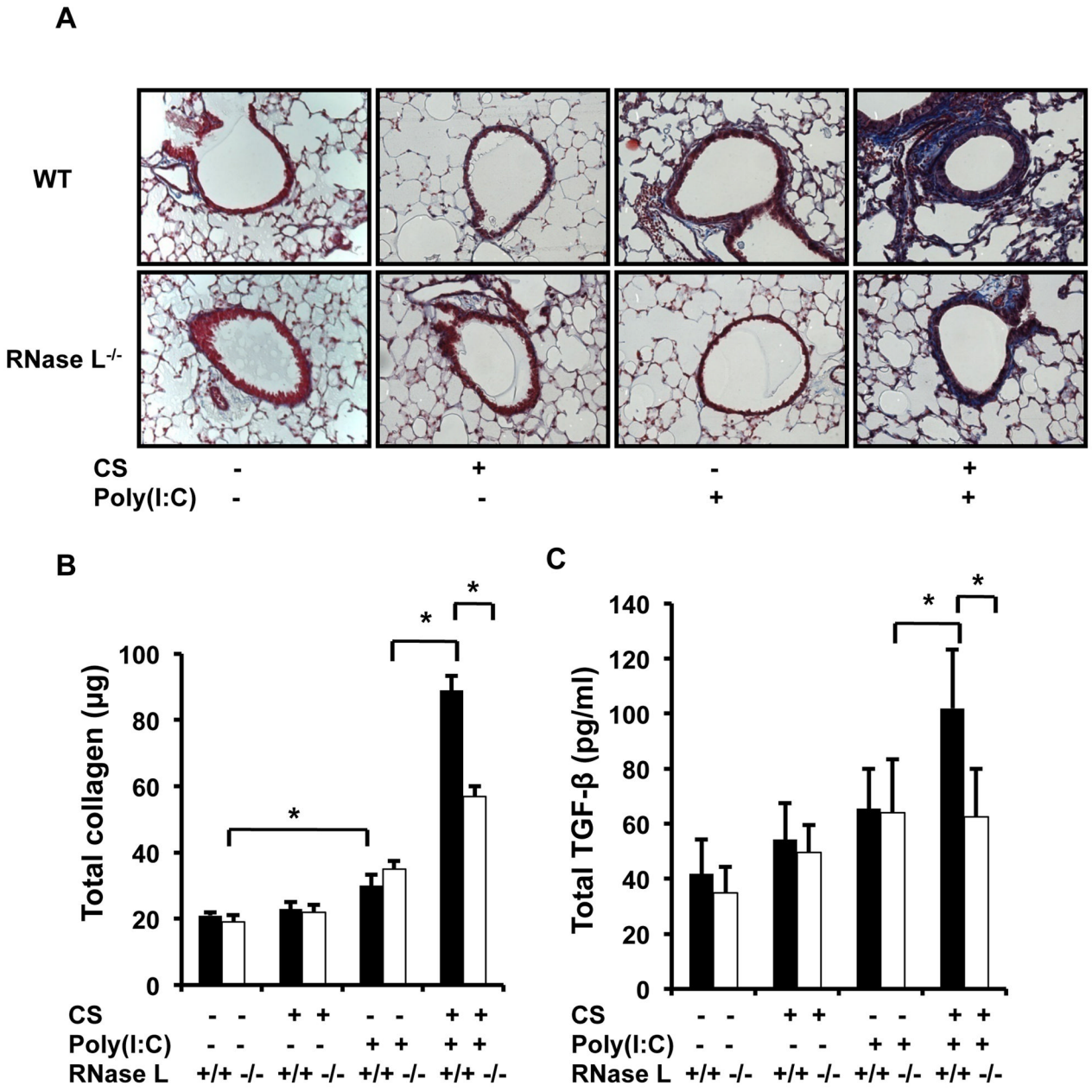

FIGURE 4.

Role of RNase L in the airway fibrosis and TGF-β1 production in lungs from mice exposed to CS plus Poly(I:C), alone and in combination. WT or RNase $L^{-/-}$ mice were exposed to CS(+) or room air (CS−) and randomized to receive Poly(I:C) or vehicle. In (A), lungs were sectioned and underwent trichrome staining. In (B), lung collagen was measured using Sircol evaluations. In(C) total BAL TGF-β1was measured by ELISA. The sections in A are representative of evaluations in a minimum of 8 mice each. The values in B and C represent the mean +/− SEM of evaluations in a minimum of 4 mice. * P≤0.05

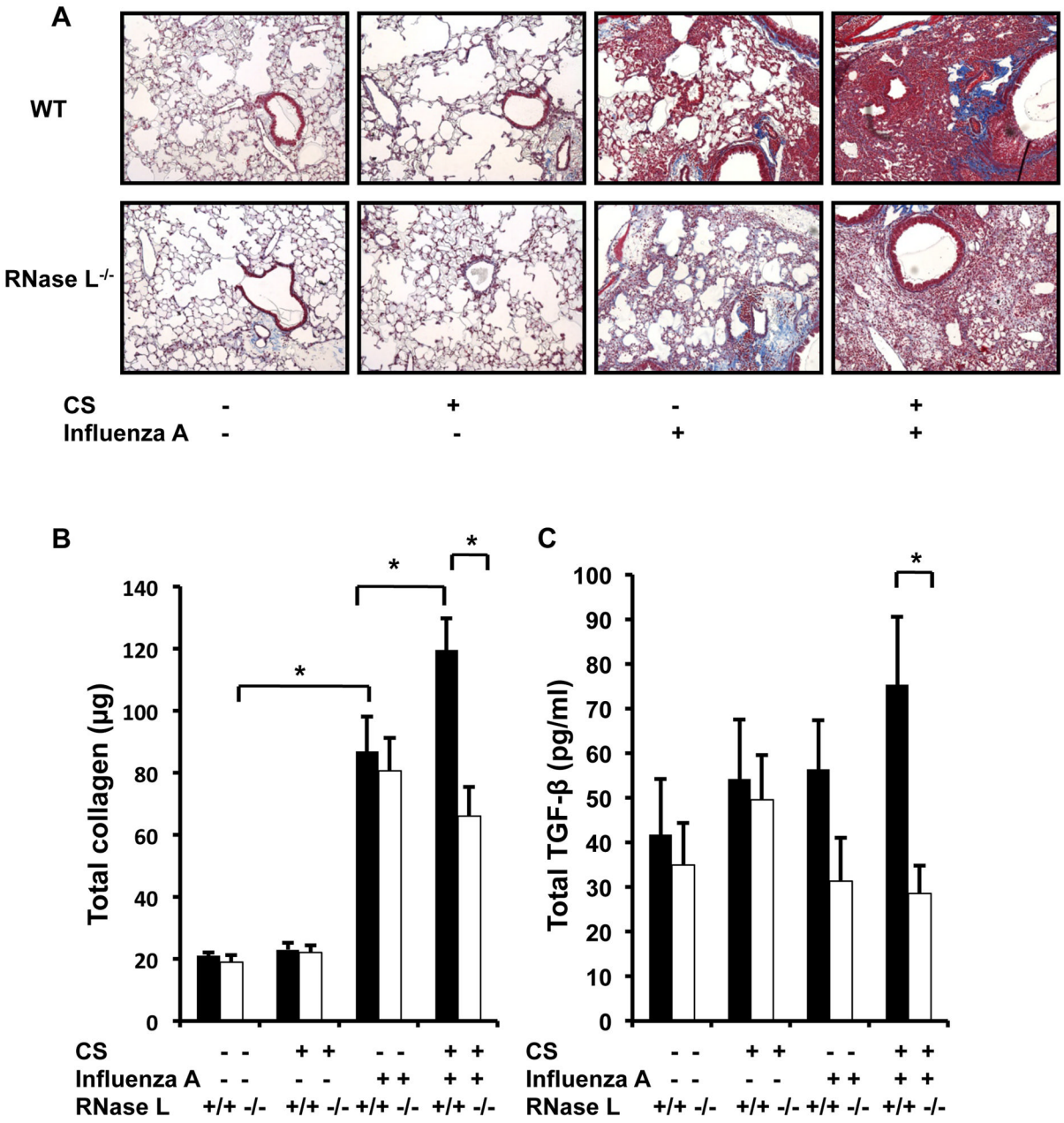

FIGURE 5.

Role of RNase L in the airway fibrosis and TGF-β1 production in lungs from mice exposed to CS plus flu virus, alone and in combination. WT or RNase $L^{-/-}$ mice were exposed to CS(+) or room air (CS−) and randomized to receive Influenza A virus or vehicle. In (A), lungs were sectioned and underwent trichrome staining. In (B) lung collagen content was measured using Sircol evaluations. In (C) total BAL TGF-β1 was measured by ELISA. The sections in A are representative of evaluations in a minimum of 8 mice each. The values in B and C represent the mean +/− SEM of evaluations in a minimum of 4 mice. * P≤0.05

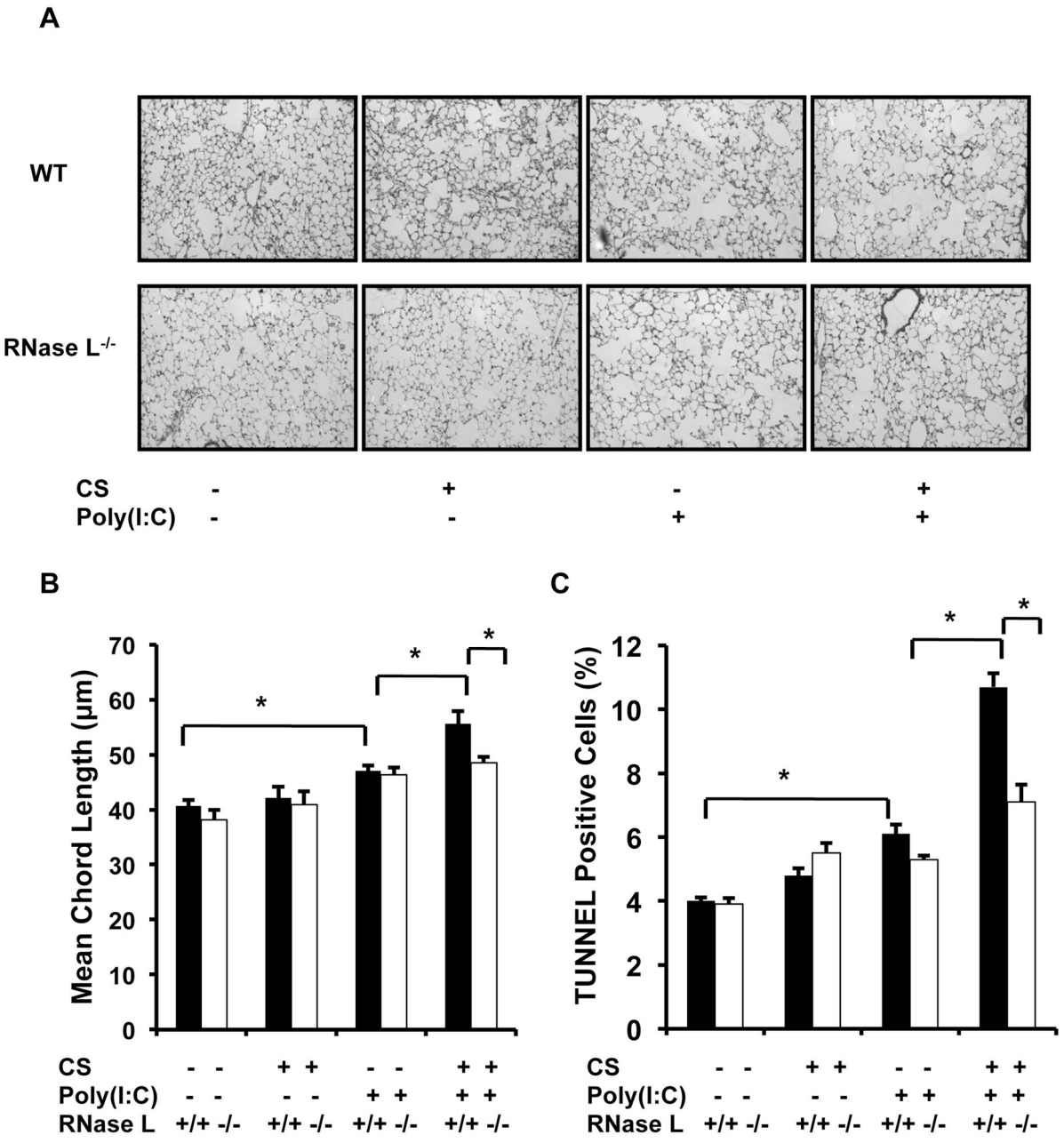

FIGURE 6.

Role of RNase L in the alveolar destruction in lungs from mice exposed to CS plus Poly(I:C), alone and in combination. WT and RNase $L^{-/-}$ mice were exposed to CS(+) or room air (CS−) and were randomized to receive Poly(I:C) or vehicle. In (A) lungs were infused with fixative under constant pressure (25 cm H_2O), sectioned and underwent H & E staining. Each section is representative of evaluations in eight mice with the noted genotype. In (B) alveolar airspace size was calculated using ImageJ analysis software. Data represent the mean +/− SEM of chord length evaluations in a minimum of 4 mice. *, P≤0.05. In (C) lungs were processed for TUNEL staining and TUNEL-positive cells were counted. The data are presented as the mean TUNEL scores ± SEM. *, P≤ 0.05.

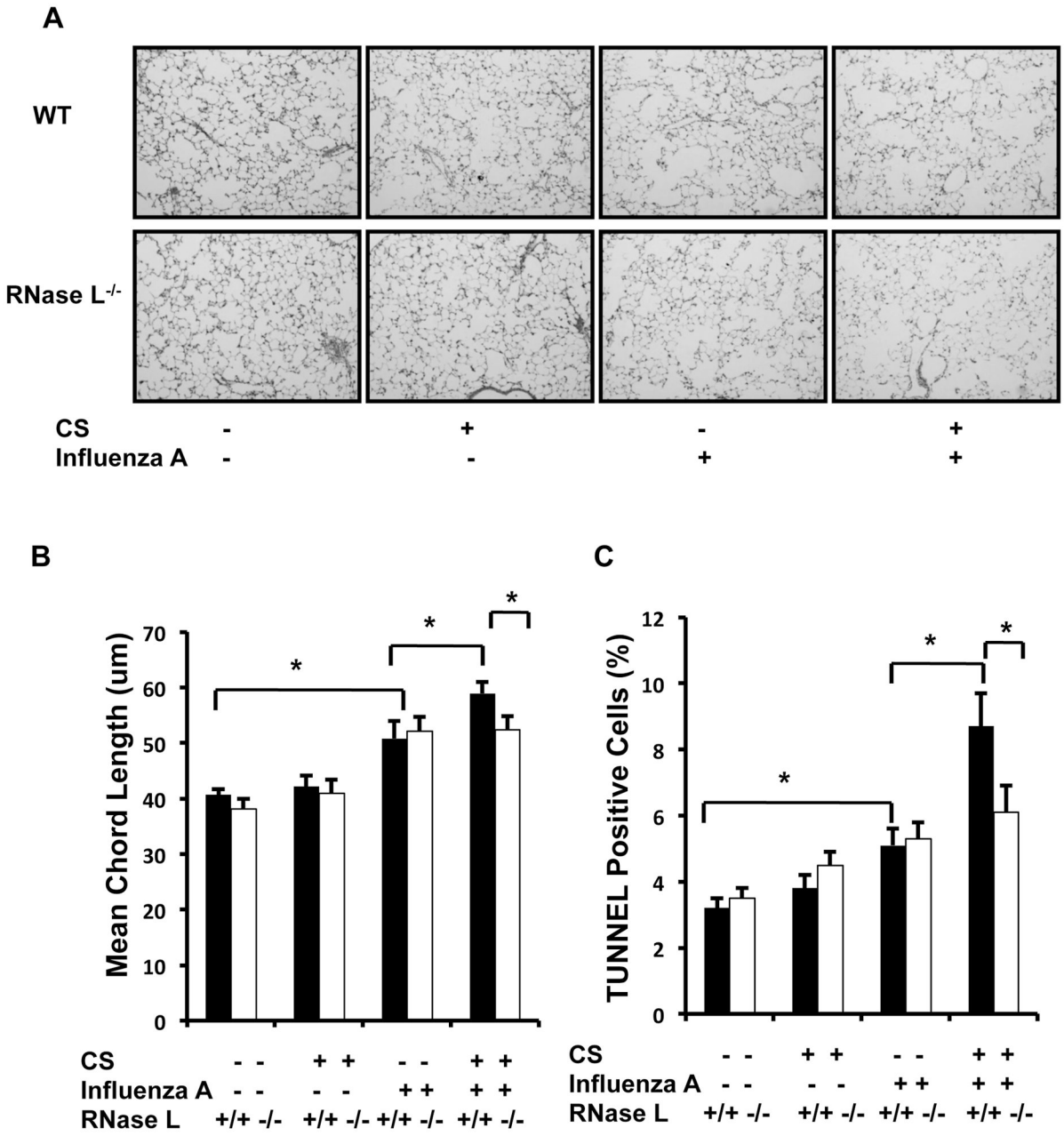

FIGURE 7.

Role of RNase L in the alveolar destruction in lungs from mice exposed to CS plus virus, alone and in combination. WT or RNase $L^{-/-}$ mice were exposed to CS(+) or room air (CS −) and randomized to receive Influenza A virus or vehicle. In (A) lungs were infused with fixative under constant pressure (25 cm H2O), sectioned and underwent H & E staining. Each section is representative of evaluations in eight mice with the noted genotype. In (B) alveolar airspace size was calculated using ImageJ analysis software. The data represent the mean +/− SEM of chord length evaluations in a minimum of 4 mice. *, P≤ 0.05. In (C), lungs were processed for TUNEL staining and TUNEL-positive cells were counted. The data are presented as the mean TUNEL scores ± SEM. *, P≤ 0.05.

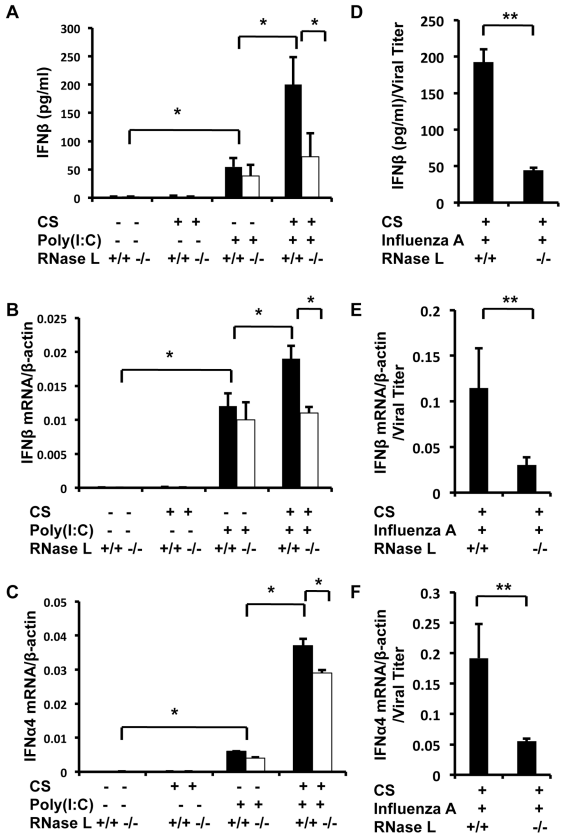

FIGURE 8.

Role of RNase L in the production of Type I Interferon in lungs from mice exposed to CS plus Poly(I:C) or influenza A, alone or in combination. WT or RNase $L^{-/-}$ mice were exposed to CS (+) or room air (CS−) and randomized to receive Poly(I:C) or influenza A or vehicle. Type I Interferon mRNAs and proteins were measured with RT-PCR and ELISA respectively. In (A) BAL IFN-β was assessed by ELISA. In (B) IFN-β mRNA levels were measured in whole-lung RNA extracts. In (C) IFN-α4 mRNA levels were measured in whole-lung RNA extracts. In (D) the levels of BAL IFN-β were assessed by ELISA and normalized to viral titer. In (E) IFN-β mRNA levels were measured in whole-lung RNA extracts and were normalized to viral titer. In (F), IFN-α4 mRNA levels were measured in whole-lung RNA extracts and were normalized to viral titer. The data in panels A and D represent the mean +/− SEM of evaluations in a minimum of 4 mice. *, P≤0.05, **, P≤0.01. The data in panels B, C, E and F are expressed as the mean +/− SEM percentage of concurrently evaluated β-actin transcripts. n = 4 for each. *, P≤0.05. **, P≤0.01.